Analysis in Mooring Chain Links Tensioned on Curved Surface

Evilly R. H. da Silveira[1], Fábio J. C. da Silva Filho[1], Michele A. L. Martins[1], Eduardo N. Lages[1], Mauro C. Oliveira[2]

[1]*Scientific Computing and Visualization Laboratory, Federal University of Alagoas*
Cidade Universitária, 57072-970, Maceió/AL, Brazil
evilly.silveira@ctec.ufal.br, fabio.filho@ctec.ufal.br, micheleagra@lccv.ufal.br, enl@lccv.ufal.br
[2]*CENPES/PETROBRAS*
Av. Horácio Macedo, 950 - Cidade Universitária da Universidade Federal do Rio de Janeiro, 21941-915, Rio de Janeiro/RJ, Brazil
mauro@petrobras.com.br

Abstract. The development of offshore energy resources, specifically oil and gas, is increasing. Consequently, there is an increasing demand for state-of-the-art technologies and concepts to enhance productivity in this sector. One critical component of deep and ultra-deep water floating platforms is the mooring system, which requires rigorous design considerations. The motivation behind this lies in the substantial repair costs associated with unexpected failures. While extensive studies have been conducted in this area, the impact of mooring equipment with curved surfaces – responsible for guiding or restricting the upper end of mooring lines – on chain link behavior remains somewhat overlooked. This study investigates the effects of ungrooved curved surfaces on the stress distribution of tensioned offshore mooring chain links. Using Finite Element Analysis (FEA), we analyze the behavior of mooring chain links when subjected to tension on curved surfaces. Our findings identify stress hotspots and calculate the corresponding Stress Concentration Factors (SCFs). Additionally, we explore the effects of changes in the radius of the curved surface. Notably, the presence of curved surfaces significantly influences stress distribution of mooring chain links, and the corresponding SFCs. These results have important implications for the design of mooring systems used in oil and gas exploration and production.

Keywords: offshore mooring, curved surface, stress distribution.

1 Introduction

Over the years, the discovery of vast oil and gas reserves in deeper waters has been attributed to the increased use of floating offshore structures in exploration and production activities [1]. The operation of these offshore installations depends on the integrity of their mooring systems. A critical component of these floating platforms, especially in deep and ultra-deep waters, is the mooring system, which requires stringent design considerations due to the substantial repair costs associated with unexpected failures.

Offshore mooring systems are designed to ensure the safety of platforms at specific operating locations. Mooring chain links are essential components commonly used in these systems [2]. Various types of mooring equipment, e.g., mooring chain windlasses, mooring chain wheels, and mooring chocks, are used to guide or restrain the upper end of mooring lines [3]. These pieces of equipment provide a curved surface for interaction with the chain links.

The fatigue of mooring chain links is estimated using a model with straight line chain links geometry under pure tension, as recommended by Bureau Veritas [4], disregarding objects connected to the mooring chain links. This assumption can influence the accuracy of the fatigue life result. Luo et al. [5], Xue et al. [3], and Barros et

al. [6] conducted studies on mooring chain links in contact with curved surfaces and pointed important effects produced by curved surfaces. However, research on mooring chain links under tension on curved surface is relatively limited.

According to Bureau Veritas [4], the estimation of combined fatigue in mooring chain links involves performing Finite Element Analysis (FEA) calculations to determine Stress Concentration Factors (SCFs). This paper examines the behavior of mooring chain links when subjected to tension on curved surfaces using FEA. The study aims to identify the impact of this interaction on stress hotspots and calculate the corresponding SCFs. It also evaluates how variations in the curved surface's radius affect the system's stress distribution.

2 Analysis of Finite Element Method

In this session, we present the details of the finite element model of the chain links assembly with a curved surface, developed using ABAQUS CAE.

2.1 Problem modeling

A simplified chain links assembly with a curved surface was modeled in ABAQUS CAE to investigate the impact of geometry on the stress distribution of the links. The assembly consists of the following parts: a curved surface, and a chain composed of three complete links and two semi-links. The semi-links are responsible for the beginning and end of the chain links assembly. Figure 1 shows each of the parts that form the assembly.

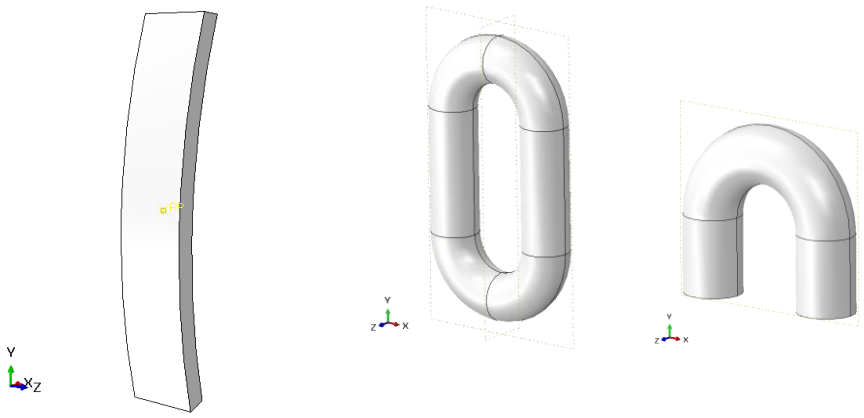

a) b) c)

Figure 1. Assembly parts: a) Curved Surface. b) Link. c) Semi-link.

To reduce the computational cost, the curved surface was modeled as a rigid body, and the analysis was performed on the set of chain links. To investigate the variations in the radius of the curved surface, surfaces with radii of 3035 mm, 3535 mm, 4535 mm, and 5035 mm were considered. The links have pre-defined dimensions according to normative guidelines, in addition to the dimensions that depend on the diameter of the cross-section. For the simulation, a diameter of 105 mm was adopted.

After modeling the components and performing the assembly, contact conditions were applied between the parts. The type of contact applied between the links and between the links and the surface was the surface-to-surface type. The sliding formulation considered was for large displacements, and the discretization method adopted was also surface-to-surface. The contact properties applied were normal and tangential. The "Hard" type was used for normal contact, with the contact constraint imposition method set to "Penalty". In addition, the option to allow separation after contact was enabled. In the case of tangential contact, the friction formulation was considered frictionless.

2.2 Material properties

The SCFs are evaluated by considering two material behaviors: linear elastic and elastoplastic, modeled by a Ramberg-Osgood law consistent with the quality of offshore steel grade R3. The main material characteristics are presented in Tab. 1.

Table 1. Properties of grade R3 offshore steel.

Mechanical properties	Symbol	Values
Young's Modulus	E [GPa]	210.0
Initial yield stress	σ_{y0} [MPa]	610.0
Ultimate stress	σ_u [MPa]	813.0
Ultimate strain	ε_u [%]	11.33

2.3 Service loading and boundary conditions

Figure 2 shows all the chain links with the curved surface assembled and finite element mesh. Two reference points, RP and RP-1, were used to apply the load and boundary conditions.

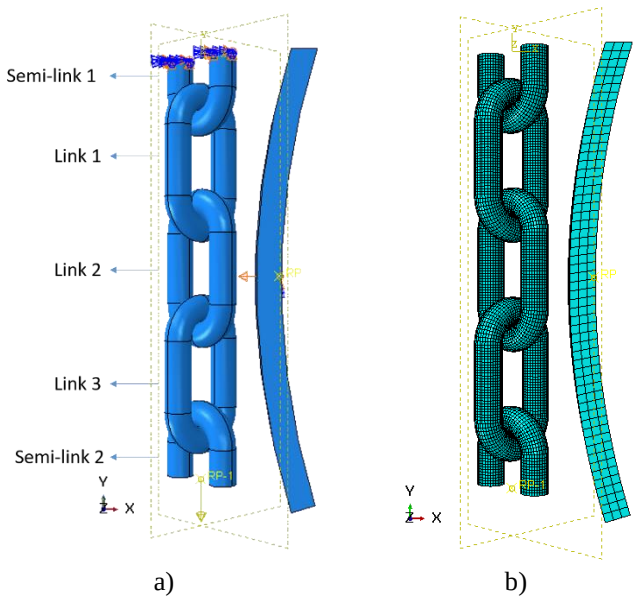

Figure 2. Modeling module: a) Assembly. b) Mesh.

The loading sequence for the model is defined in two phases: manufacturing and operation. In the manufacturing phase, the mooring is subjected to a proof load corresponding to 70% of the minimum breaking load [7]. The proof load value in kilonewtons, according to DNVGL [7], considering the model material, is obtained by

$$P_f = 0.0156\, d^2\, (44 - 0.08\, d). \tag{1}$$

The proof load corresponds to 6122.84 kN, and the operational load applied corresponds to 1727.50 kN. Figure 3 illustrates the loading sequence used during the simulation, where the step from 0 to 1 represents the application of the proof load, followed by unloading (1-2). In the step from 2 to 3 the operational load is applied. Finally, the operational load is kept constant in the remaining steps (3-4 and 4-5).

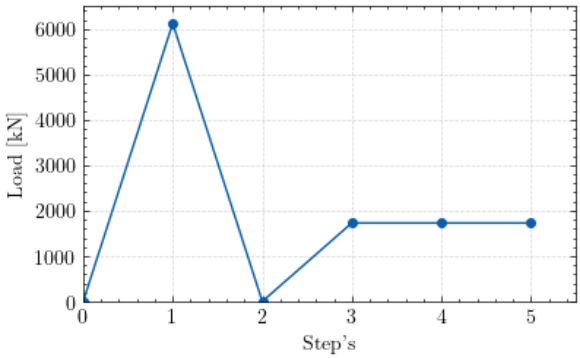

Figure 3. Load at each step.

Boundary conditions are constraints applied to the modeling to represent the expected behavior of the system. In the model studied in this paper, five boundary conditions were used, designated as BC-1, BC-2, BC-3, BC-4, and BC-5, each defined by properties: BC-1 refers to a Displacement/Rotation condition applied to the fixed link, with displacement restricted in the X and Z planes; BC-2 is a Symmetry/Antisymmetry/Fixed condition also applied to the fixed link, where displacement restricted in the Y plane, and rotations are restricted in the X and Z planes; BC-3 involves a Displacement/Rotation condition applied to point RP-1, with rotation prescription along the Z axis; BC-4 is a Displacement/Rotation condition applied to point RP, with displacement along the X axis prescribed on the curved surface for contact with the links during the operation phase; and BC-5 is a Displacement/Rotation condition applied to point RP, with displacement restricted on the curved surface for all degrees of freedom. Table 2 summarizes the defined boundary conditions along the steps. The initials represent creation “C”, propagation “P” and inactive “I”.

Table 2. Boundary conditions along the steps.

BCs	Initial	Step-1	Step-2	Step-3	Step-4	Step-5
BC-1	C	P	P	P	P	P
BC-2	C	P	P	P	P	P
BC-3	-	-	-	-	-	C
BC-4	-	-	-	-	C	I
BC-5	-	-	-	-	-	C

2.4 Finite element mesh

The element type selected for the set of links is C3D8R, hexahedral finite elements with eight nodes and reduced integration, the standard element suggested by the program for this type of simulation. The approximate global size of each element is parameterized to have 10% of the diameter of the link. For the curved surface, the quadrilateral rigid element R3D4 was adopted, with the global size parameterized to be 10% of the height of the surface section. Figure 4 presents detailed information about the mesh used.

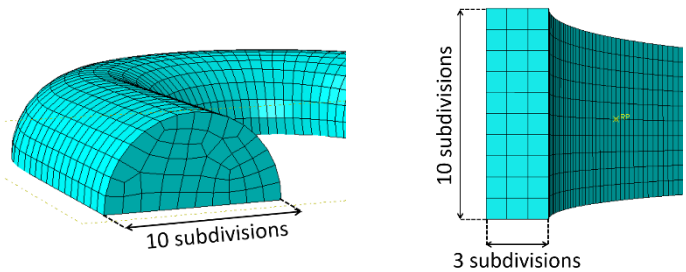

a) b)

Figure 4. Mesh detailing: a) Link. b) Curved surface.

3 Estimation of SCF in Chain Links using Finite Element Method

The Stress Concentration Factors (SCF) are estimated through Finite Element Method (FEM) calculations to obtain the stresses and calibrated through full scale model tests of chain links [4]. Disregarding the effects of corrosion, the SCF for pure tension is calculated using the equations:

$$SCF_{TT} = \frac{\sigma_{TT}}{\sigma_{TT,nom}}, \tag{2}$$

$$\sigma_{TT,nom} = \frac{2T}{\pi d^2}, \tag{3}$$

where σ_{TT} refers to the maximum principal stress due to pure tension obtained from the FEA analysis, $\sigma_{TT,nom}$ represents the nominal stress, with T the tension applied to the set of links, and d is the chain diameter.

Regions considered critical for chain link fatigue are those known for experiencing high stress rates [8]. If a defect appears in these regions, it can lead to crack initiation during subsequent load cycles. This localized stress may result in crack propagation, increasing the risk of fatigue damage [9].

4 Results and discussion

The results presented in this section refer to the link in contact with the load application semi-link (Link 3), which has a more significant interaction with the curved surface. Figure 5 illustrates the stress distribution to the link subjected to pure tension at the end of Step 3, where there is no interaction between the chain links and the ungrooved curved surface.

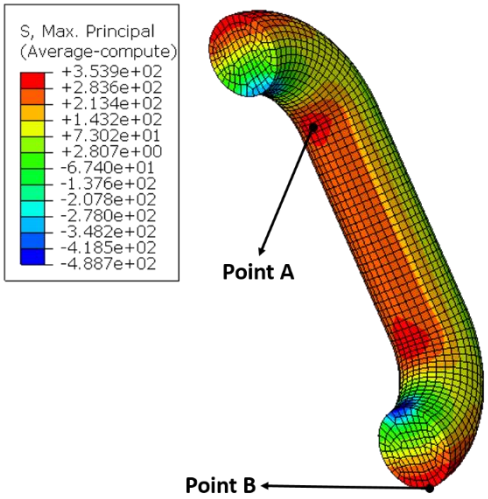

Figure 5. Stress distribution link 3 subjected to pure traction

The stress hotspots are located on the outer side of the crown and the inner side of the curvature. These findings align with previous studies, such as Rampi et al. [10]. Table 3 shows the stress concentration factors for the two locations: the inner side of the curvature (Point A) and the outer side of the crown (Point B).

Table 3. SCFs of link 3 subjected to pure traction without interaction with an ungrooved curved surface.

Point	$\sigma_{TT,nom}$ [MPa]	σ_{TT} [MPa]	SCF_{TT}
Point A	99.75	338.197	3.390
Point B	99.75	353.900	3.548

The stress concentration factor on the outer side of the crown is greater than at the inner point of the curvature, indicating a greater stress concentration at this specific point for the situation where the set of links is not in contact with the curved surface.

Four surfaces with radii of 3035 mm, 3535 mm, 4535 mm, and 5035 mm were analyzed to investigate the impact of the interaction between the set of links and the curved surface. As illustrated in Fig. 6, the geometry significantly impacts the stress distribution of the links.

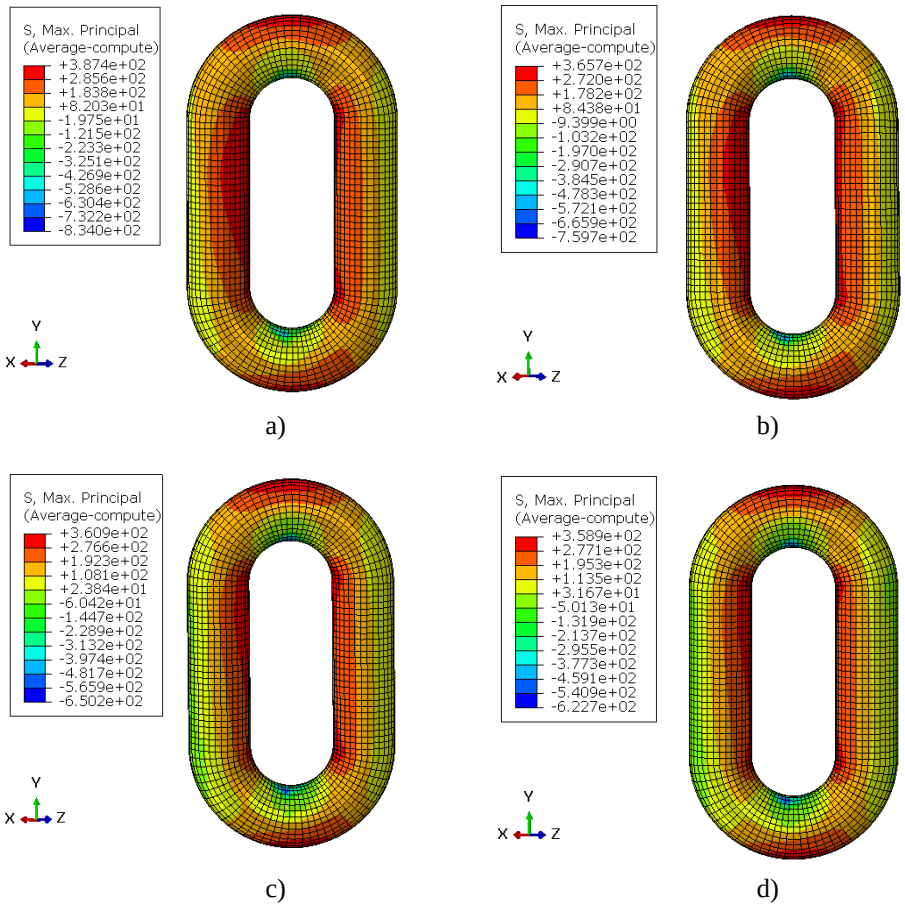

Figure 6. Stress distribution of link 3 at the end of Step 5 for curved surfaces with radius: a) 3035 mm. b) 3535 mm. c) 4535 mm. d) 5035 mm.

The regions of greatest stress concentration are found in the straight segment of the link in contact with the curved surface at the end of Step 5. As a result, the maximum stress values are concentrated in these specific areas. Furthermore, it is observed that the magnitudes of the maximum and minimum stresses decrease as the radius of the curved surface increases. The values of SCF for different surface radii are presented in Tab. 4.

Table 4. SCFs of link 3 subjected to pure tension with interaction with an ungrooved curved surface.

Radius [mm]	$\sigma_{TT,nom}$ [MPa]	σ_{TT} [MPa]	SCF_{TT}
3035	99.75	387.355	3.883
3535	99.75	362.325	3.632
4535	99.75	355.192	3.561
5035	99.75	354.821	3.557

Notably, as the radius of the curved surface increases, the stress concentration factor decreases. Furthermore, the concentration factors obtained using a curved surface with a radius of 3035 mm are higher than the stress concentration factors determined for the pure tension scenario, where the interaction between the chain links and

the surface is not considered. Therefore, the presented results confirm that the curved surface significantly influences the stress distributions in the links and the stress concentration factors.

5 Conclusions

This study offers a significant contribution to understanding the behavior of chain links in contact with curved surfaces, an aspect often neglected in traditional analyses of offshore mooring systems. Through Finite Element Analysis (FEA), it was possible to identify the stress hotspots in chains subjected to tension on ungrooved curved surfaces, and to evaluate the impact of different radii of these surfaces on the stress distribution. The results demonstrate that curved surfaces substantially affect the stress distribution in the anchor chains and the corresponding stress concentration factors. Furthermore, it was observed that increasing the radius of the curved surface reduces the stress concentration factors. These findings have important practical implications for designing and maintaining mooring systems on offshore platforms, especially in deep and ultra-deep waters, where failures can entail high costs and significant risks. Future work may explore fatigue analysis using S–N curves, the inclusion of curved surfaces with grooves, the application of different levels of operational traction, and the consideration of friction between links, expanding the applicability and robustness of the presented results.

Acknowledgements. The authors acknowledge PETROBRAS and CNPq for the financial support.

Authorship statement. The authors hereby confirm that they are the sole liable persons responsible for the authorship of this work, and that all material that has been herein included as part of the present paper is either the property (and authorship) of the authors, or has the permission of the owners to be included here.

References

[1] I. A. Ja'e, M. O. A. Ali, A. Yenduri, Z. Nizamani and A. Nakayama, "Optimisation of mooring line parameters for offshore floating structures: A review paper". *Ocean Engineering*, v. 247, p. 110644, 2022.
[2] J. Lee, G. T. Tayyar, J. Choung. "In-plane and out-of-plane bending moments and local stresses in mooring chain links using machine learning technique". *International Journal of Naval Architecture and Ocean Engineering*, v. 13, p. 848-857, 2021.
[3] X. Xue, N. Chen, Y. Pu; L. Chen and L. Wang, "Fracture mechanics assessment for mooring chain links tensioned over a curved surface". *Applied Ocean Research*, v. 117, pp. 102900, 2021.
[4] Bureau Veritas, "Fatigue of Top Chain of Mooring Lines due to In-Plane and Out-of Plane Bendings", Guidance Note NI 604 DT R00 E, 2014.
[5] M. Luo and C. Heyl, "Numerical study on the out-of-plane bending (OPB) behaviors of studless mooring chain links in fairlead structures". *International Ocean and Polar Engineering Conference*, pp. 1105-1112, 2017.
[6] L. O. Barros, F. A. Hansen, R. S. Neves, G. V. Ferreira, L. L. D. Morales and L. Malcher, "Fatigue life estimate of metallic chain links of mooring systems assuming out of plane bending: From constant amplitude to random loading". *Ocean Engineering*, v. 288, pp. 116139, 2023.
[7] DNV GL. Offshore standard – offshore mooring chain (DNVGL-OS-E302), Edition July 2018, 2018.
[8] K. Berthelsen. Out of plane bending of mooring chains - finite element analysis of a 7-link model. Master's Thesis, Norwegian University of Science and Technology, 2017.
[9] P. Bastid, and S. D. Smith, "Numerical analysis of contact stresses between mooring chain links and potential consequences for fatigue damage", Proceedings of the ASME 2013 32nd International Conference on Ocean, Offshore and Arctic Engineering (OMAE2013-11360), 2013.
[10] L. Rampi, F. Dewi and P. Vargas, "Chain out of plane bending (OPB) Joint Industry Project (JIP) summary and main results", Offshore Technology Conference 2015 (OTC-25779-MS), 2015.